Observed aerosol and liquid water path relationships in marine stratocumulus

Xue Zheng,[1] Bruce Albrecht,[1] Patrick Minnis,[2] Kirk Ayers,[2] and Haflidi H. Jonson[3]

Received 26 May 2010; revised 12 July 2010; accepted 28 July 2010; published 15 September 2010.

[1] The stratocumulus-topped marine boundary layer (BL), aerosol, and cloud properties observed on research flights made off the coast of northern Chile in the Southeastern Pacific (20°S, 72°W) during the VAMOS Ocean-Cloud-Atmosphere-Land Study-Regional Experiment (VOCALS-REx) were used to examine the variation of liquid water path (LWP) and cloud condensation nuclei (CCN). Ten flights were made under similar meteorological conditions where the BL structure was well-mixed, clouds were solid, and the conditions at the surface and at the top of the BL were similar. A strong positive correlation between the LWP, which varied from 15 to 73 gm^{-2}, and the BL CCN, which ranged from 190 to 565 cm^{-3}, was observed. Analysis of the highest and the lowest CCN concentration cases confirms that the differences in the thermodynamic jumps at the top of the BL and the turbulent fluxes at the surface cannot explain the observed differences in the LWP. Cloud properties from satellite retrievals combined with a back trajectories analysis demonstrated that the LWP differences observed at the time of the aircraft flights are also prevalent during the night-time hours prior to the aircraft observations. These results provide evidence for CCN and LWP relationships that are not fully explained by current hypotheses from numerical modeling. **Citation:** Zheng, X., B. Albrecht, P. Minnis, K. Ayers, and H. Jonson (2010), Observed aerosol and liquid water path relationships in marine stratocumulus, *Geophys. Res. Lett.*, *37*, L17803, doi:10.1029/2010GL044095.

1. Introduction

[2] Anthropogenic aerosol particles are considered to modify marine stratocumulus cloud (Sc) properties by suppressing drizzle processes, which could increase cloud amount, lifetime, and liquid water path (LWP) [*Albrecht*, 1989]. This indirect effect has controversial aspects and caveats that are revealed by numerical simulations [e.g., *Lu and Seinfeld*, 2005; *Hill and Feingold*, 2009] and satellite-based observations [*Coakley and Walsh*, 2002; *Brioude et al.*, 2009]. Current hypotheses from large-eddy simulations (LES) [*Ackerman et al.*, 2004; *Bretherton et al.*, 2007; *Hill and Feingold*, 2009] propose that the inhibited sedimentation due to reduced cloud droplet size, and the enhanced evaporation and entrainment at the cloud top reduces LWP by 10% in the polluted clouds. *Wood* [2007] used a mixed layer model to show that entrainment was enhanced in polluted clouds with high cloud bases resulting in a thinning of the cloud that was more significant than drizzle reduction in LWP during the first 24 hours of simulations.

[3] There are two main challenges for observations [*Stevens and Feingold*, 2009]. First, satellite observations of aerosols are limited in cloudy regions. Further, in some cases it is difficult to use satellite observations to distinguish between cloud droplets and aerosols [*Koren et al.*, 2007]. Second, for both satellite and in situ measurements, meteorological factors can also control the variation of cloud water content [*Stevens and Feingold*, 2009; *Painemal and Zuidema*, 2009; *George and Wood*, 2010]. This study uses in-situ aircraft and remote satellite observations to investigate the relationship between cloud LWP and cloud condensation nuclei (CCN) concentration in Sc under relatively constant meteorological conditions.

2. Data and Methods

[4] Observations for this study were made using the CIRPAS Twin Otter aircraft on 18 flights over the subtropical southeastern Pacific at a fixed location (20°S, 72°W;designated Point Alpha) during VOCALS-REx from Oct.16 to Nov.13 2008. Instruments on the aircraft measured standard meteorological variables, turbulence, aerosol, cloud, and precipitation (Table 1).

[5] The cloud and boundary layer structures observed on 8 of the 18 flights included complications involving strong wind shear within the MBL, moist layers above the inversion, strong decoupled BL with cumulus below Sc. In this study, 10 remaining cases in which inversion heights varied between 1000 and 1300 m, potential temperature increased across the capping inversion in a range of 12–17°C, and total water mixing ratio decreased across the inversion in a range of 5.5 to 8 g/kg. The drizzle water contents from the Cloud Imaging Probe (CIP) on the 10 days were less than 10^{-3} g m^{-3}. Based on this analysis, the clouds occurring during these selected 10 days are assumed to exist in relatively similar meteorological conditions, although the sea-surface temperature (SST) at Alpha increased from 16.5–19.3°C during the course of the study. Therefore, the influences of meteorological factors (including coastal effects) are assumed to be minimal. The majority (7) of the ten flights were made around 0900 Local Time (LT) (1200 UTC), while the others were conducted from around 1200 to 1300 LT.

[6] The thermodynamic structures for these flights are shown in Figure 1 using a height scale normalized by the inversion height. These structures show well-mixed BL capped by sharp inversions and similar BL thermodynamics for all the cases selected. The cloud thicknesses and liquid water contents, however, for these cases vary substantially among the 10 cases.

[1]Division of Meteorology and Physical Oceanography, Rosenstiel School of Marine and Atmospheric Science, University of Miami, Miami, Florida, USA.
[2]NASA Langley Research Center, Hampton, Virginia, USA.
[3]Naval Postgraduate School, Monterey, California, USA.

Copyright 2010 by the American Geophysical Union.
0094-8276/10/2010GL044095

Table 1. Instrumentations of Aerosol, Clouds and Precipitation Probes

Instrument	Observations	Variables
Gerber Probe	Liquid water	LWC
Cloud Imaging Probe (CIP)	Drizzle droplet size range: 25–1500 μm	Drizzle water content
CCN Spectrometer	CCN at 0.2% super–saturation	CCN
Passive Cavity Aerosol Spectrometer Probe (PCASP)	Aerosol size range: 0.1–2 μm	Accumulation mode Aerosol concentration
Cloud, Aerosol and Precipitation Spectrometer (CAPS)	Cloud droplet size range: 2.07–40.2 μm	Cloud droplet concentration

[7] For each flight day, all CCN measurements (at a supersaturation of 0.2%) below cloud base and within 50 km of Point Alpha are averaged to give mean CCN concentrations. The sub-cloud and above-inversion PCASP accumulation mode aerosol concentrations (PCASP concentrations hereafter) in the sub-cloud layer and cloud droplet concentrations (Nc) in the cloud layer are calculated in a similar way. The sounding of liquid water content (LWC) from the Gerber probe is integrated to estimate LWP. The LWC from the soundings and the horizontal leg averages at different levels have mean difference for all flights of 0.03 ± 0.04 gm^{-3}, indicating that the LWC from soundings are representative of the larger-scale cloud area. Vertical velocity observations (at 40 Hz) are used to calculate the vertical velocity variance along the horizontal 10-minute legs at different levels. To further analyze the history of the air masses sampled by the aircraft, we use the Hybrid Single Particle Lagrangian Integrated Trajectory Model (HYSPLIT) model [*Draxler and Rolph*, 2003] driven with the NCEP Global Data Assimilation System (GDAS) data to calculate the backward and forward trajectories starting at Point Alpha and the 500-m level for 36 hours forward and backwards. In addition, radiances from the Tenth Geostationary Operational Environmental Satellite (GOES-10) were used to retrieve cloud properties using the methods of *Minnis et al.* [2010a, 2010b] for areas in the vicinity of the aircraft measurements and at times prior to and after the measurements along the HYSPLIT trajectories.

3. Results

[8] The CCN concentrations in the sub-cloud layer varied from 190 to 565 cm^{-3} among the 10 flights and were positively correlated with Nc, which ranged from 188 to 392 cm^{-3}. The LWPs in these relatively thin clouds ranged from 15 to 73 gm^{-2} and are positively correlated with the aerosol and Nc (Figure 2). The LWP estimated from the GOES analyses are also shown in Figure 2. The average difference between the aircraft and satellite (50 km) LWP is −4.9 ± 13 gm^{-2}. These results further support the idea that the sounding estimates of the LWP are representative of a larger area as viewed by the satellite.

[9] The positive correlation between the CCN concentrations and Nc are shown in Figure 3 where the probe concentrations are sorted from lowest to highest CCN concentrations. The correlation between the CCN (and PCASP), and Nc is evident, although the deviation between the CCN and Nc increases with increasing CCN (and PCASP) concentrations. The PCASP concentrations above the inversion are lowest when the Nc are high and indicate no major influence of the above-inversion aerosols on the BL aerosol conditions.

[10] Backward trajectories for 9 of the 10 flights indicate a flow from the southeast of Point Alpha from points close to the coast of Chile 36 hours earlier. During the 36 hour periods, 6 of the air masses moved less than 500 km and remained over water, while the air masses for the other 2 cases (Oct16 and 18) moved about 900 km from the south. The SST isotherms in this area are oriented southeast to northwest, and since the synoptic patterns for the cases are similar, advective effects did not vary substantially from case to case as indicated by the similar trajectories on all but one case. The October 27 case indicates a major difference from the others in that air began its 36-h journey near the southern coast of Peru. Although there are uncertainties in these back trajectories due to errors in the GDAS, the errors should be smallest in the early history of the trajectories.

[11] To further investigate BL, aerosol, and cloud characteristics for the cases with high and low CCN concentrations, we averaged two cases (October 18 and 19) with the highest CCN (HC) and the two cases (October 27 and November 9) with the lowest CCN (LC). Characteristics of the BL, clouds, and aerosols for the HC and LC cases are given in Table 2 along with the averaged features for the highest 5 cases and the lowest 5 cases. The HC PCASP concentration is about double that for the LC cases, which is consistent with the CCN values. The higher CCN concentrations for the HC cases are associated with Nc of 376 cm^{-3}, which are 153 cm^{-3} higher than that in the LC case. Both the mean in-situ LWP and the mean GOES LWP within a 20-km radius circle around Point Alpha are higher for the HC (65 gm^{-2} and 75 gm^{-2}) cases compared to those for the LC (18 gm^{-2} and 36 gm^{-2}) cases. The LWP difference between HC and LC is significant and larger than the data uncertainty. The SST in the HC cases is 1.8°C lower than that for LC. The lower SSTs and surface wind speeds for the

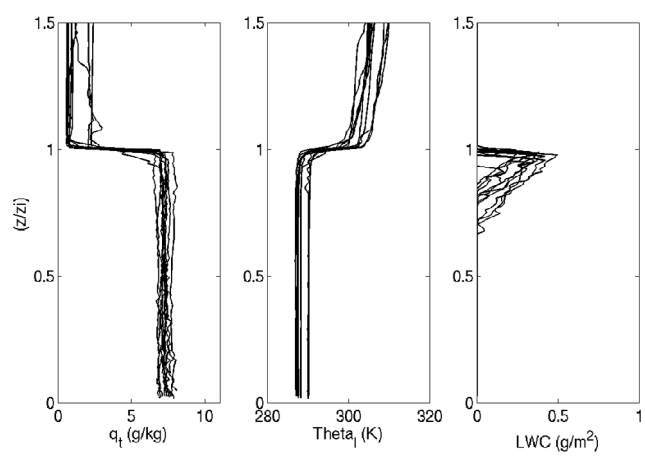

Figure 1. Vertical profiles of total water mixing ratio, liquid water potential temperature, and liquid water content for the ten cases in the study (Oct. 16, Oct. 18, Oct.19, Oct. 21, Oct. 22, Oct. 26, Oct. 27, Nov. 9, Nov. 10, Nov. 12, 2008).

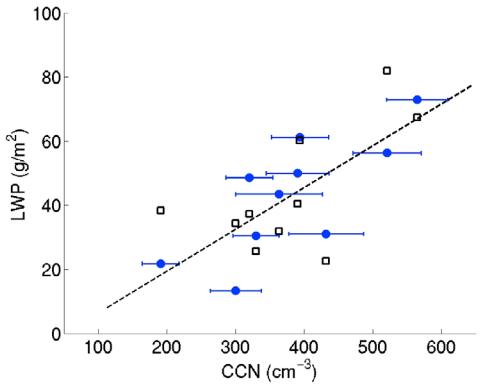

Figure 2. LWP as a function of sub-cloud CCN concentrations for selected 10 flights. Blue solid symbols are from aircraft profiles. The error bars through these symbols indicate the standard deviation of CCN. Open symbols are averages from GOES retrievals within radii of 20 km. Line is the best fit to the aircraft LWP estimates.

HC case are also associated with a surface virtual temperature flux ($F\theta_v$) that is 5.3 Wm^{-2} lower, and a water vapor flux (F_{qv}) that is 14.2 Wm^{-2} lower as well. Mixed layer theory [*Schubert et al.*, 1979] would indicate that an increase in either SST or surface wind speed would increase the cloud depth (and LWP), which is counter to the observations. The potential temperature jumps across the inversion are 15.8 K and 13.5 K for the HC and LC, respectively, and the corresponding total water mixing ratio jumps are 6.2 and 5.6 g/kg. The average HC cloud top is 138 m lower than its LC counterpart, while the HC cloud base is 240 m lower than that for the LC cases. The ratio of the observed LWP to the adiabatic LWP is about 0.79 compared with 0.61 for the LC data. Thus for the HC case the larger LWP is due to a cloud that is both thicker and closer to adiabatic than the LC cases. The averages for the 5 highest and the 5 lowest CCN cases also show similar, but somewhat reduced differences between the two cases.

[12] Compared with the LC results, the HC cases have stronger and lower inversions, which are consistent with either stronger large-scale subsidence or weaker entrainment rates. Using the eddy fluxes of total water at cloud top, the estimated entrainment rates $W_e = -\overline{(w'(q' + \ell')}/(\Delta q_t)$ are 1.1 and 1.9 mm/s respectively. Although there is substantially uncertainty in these estimates of entrainment, they suggest that the entrainment rates in the HC case are lower than those in the LC case (consistent with the lower HC inversion height), although the w variance in the cloud layer (Table 2) is 0.26 m^{2}s^{-2} for the HC case compared with 0.16 m^{2}s^{-2} in LC case, although the 5-case averages are similar.

[13] To explore the time history of the observed differences in the LWP for the HC and LC cases, the cloud properties along the back and forward trajectories from the GOES satellite retrievals are also considered. Figure 4 shows the

Table 2. Cloud, Aerosol, and BL Characteristics Averaged for the Two Cases With the Highest CCN, the Two Cases With the Lowest CCN, the Five Highest CCN Cases, and the Five Lowest CCN Cases

	HIGH CCN (2 Cases)	LOW CCN (2 Cases)	HIGH CCN (5 Cases)	LOW CCN (5 Cases)
PCASP (cm^{-3})	613	367	561	410
CCN (cm^{-3})	543	245	460	301
Nc (cm^{-3})	376	223	315	276
LWP (g/m^2)	65	18	54	32
LWP_{SAT} (g/m^2)	75	36	55	33
LWP/LWP_{adia}	0.79	0.61	0.74	0.73
SST (^{o}C)	16.7	18.5	17.7	17.7
$F\theta_v$ (W/m^2)	8.8	14.1	7.0	8.4
Fq (W/m^2)	30.4	44.6	40.5	50.9
w variance (m^{2}s^{-2})	0.26	0.16	0.18	0.17
CLD TOP (m)	1050	1188	1070	1088
CLD Base (m)	750	990	850	940
$\Delta\theta$ (K)	15.8	13.5	12.3	11.1
$-\Delta(q+\ell)$ (g/kg)	−6.2	−5.6	−6.3	−5.7
$\Delta\theta_l$ (K)	14.2	11.2	13.1	11.7
w_e (mm/s)	1.1	1.9	1.3	1.8
30m wind speed (m/s)	3.7	5.7	4.5	4.8

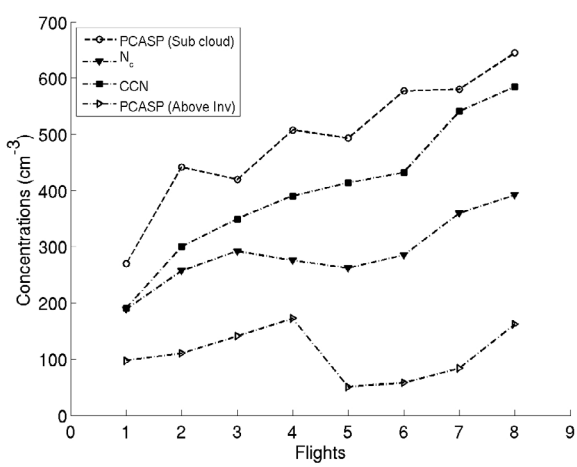

Figure 3. Sub-cloud layer CCN, PCASP and Nc for 10 cases sorted by increasing CCN from flight 1 to 10. Above-inversion PCASPs are also shown for comparison.

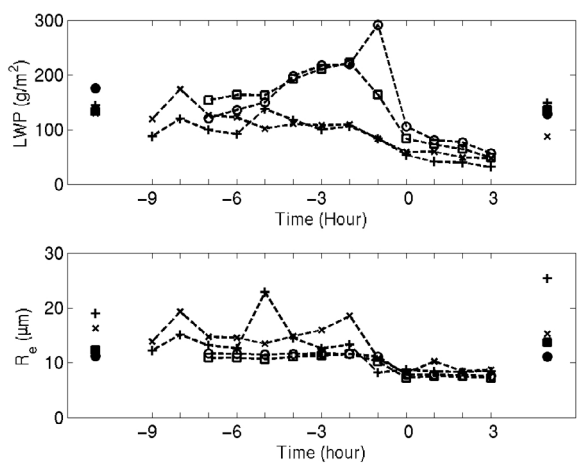

Figure 4. Time evolution of GOES-derived LWP and R_e for the two lowest (cross symbols) and the two highest (open symbols) CCN concentrations from 9 hours prior to the flight (marked as t = −9hr) to 3 hours after flight time (t = 3hr). Solid dots at left and right sides of the lines are 6-hour averaged values during midnight one day before and one later.

time evolution of LWP and cloud droplet effective radius (R_e) for the HC and LC cases from 9 hours before to 3 hours after the flights each day. The flight time for this satellite analysis is set at 1145 UTC. The LWP from the satellite retrievals decreased sharply after sunrise in all four cases, during the night the HC cases had much a much larger LWP than the LC cases. After sunrise, LWP in the HC cases decreased, but remained larger than those in the LC cases. The relatively sharp drops in LWP after sunrise, especially for the greater of the HC cases are due to the change in the satellite retrieval algorithms between day and night [*Minnis et al.*, 2010a]. Nevertheless, the nighttime algorithm shows some skill in discriminating between optically thick and thin clouds and areas with small or large droplets, especially for Sc [*Minnis et al.*, 2010b]. The time series of R_e for those four cases indicates that the HC cases had lower R_e values than those for the LC cases during the entire period. The Lagrangian analysis indicates that the differences observed by the aircraft may have existed at least 9 hours prior to the observations, which implies that the LWP differences for the extreme cases mainly resulted from cloud evolution rather than differences in external meteorological influences.

4. Summary and Discussion

[14] The MBL, aerosol, and cloud properties observed on ten research flights made off the coast of Northern Chile indicate a strong positive correlation between BL CCN concentrations and cloud LWP associated with similar BL and synoptic conditions. A detailed study of the two highest and the two lowest CCN concentration (HC and the LC cases) further confirms that the differences in the thermodynamic jumps at the top of the BL and the turbulent fluxes at the surface cannot explain the observed differences in the LWP. Satellite retrievals from GOES 10 show that the LWP differences observed at the time of the aircraft flights are also prevalent during the night-time hours prior to the aircraft observations. The positive correlation in this study is inconsistent with some of the conclusions from previous modeling studies [e.g., *Ackerman et al.*, 2004; *Bretherton et al.*, 2007; *Wood*, 2007] and satellite analyses [e.g., *Painemal and Zuidema*, 2009; *George and Wood*, 2010]. The satellite analyses investigated the climatological cloud properties over a large area of cloud deck; therefore the large scale environment variations could not be excluded. Further, in our study, the ratio of LWP and adiabatic LWP is much less than unity in some clouds, which implies that entrainment and drizzle processes prior to the observations could be forcing cloud liquid water contents to deviate from the adiabatic values. The treatment of non-adiabatic clouds may cause problems in mixed layer formulations [e.g., *Wood*, 2007]. We were unable to show that the entrainment rates for the high CCN case are significantly larger than the low CCN cases. Thus enhanced entrainment due to evaporation as shown by modeling studies (e.g., Ackerman et al. and Bretherton et al. for meteorological conditions similar to those in this study) was not a dominant process in the HC cases studied.

[15] Although we compared cases where the meteorology and the BL structure are very similar, we cannot eliminate the possibility that the changes in CCN may be associated with small changes in the large-scale forcing that in turn may also affect the LWP. True cause and effect cannot be established. Thus this work may motivate further studies to better explain the factors that control LWP and the role that the second indirect effects may play in the evolution of clouds.

[16] **Acknowledgments.** We are grateful for the dedicated efforts of several individuals in making the observations from the CIRPAS Twin Otter during VOCALS-REx. Graham Feingold and Patrick Chuang provided key scientific input on the observing strategies employed and interpretation of the initial results. Shaunna Donaher, Dione Rossiter, and Virendra Ghate, provided critical support as airborne scientists. Djamal Khelif kindly provided the high temporal resolution observations for estimating turbulence quantities. Pilots Mike Hubble and Chris McGuire skillfully executed the flight plans and endured the long ferry of the Twin Otter aircraft to Iquique Chile and back. This research was supported by ONR grant N000140810465. Patrick Minnis and Kirk Ayers were supported by the Department of Energy ARM Program through DE-AI02-07ER64546.

References

Ackerman, A. S., M. P. Kirkpatrick, D. E. Stevens, and O. B. Toon (2004), The impact of humidity above stratiform clouds on indirect aerosol climate forcing, *Nature*, *432*, 1014–1017, doi:10.1038/nature03174.

Albrecht, B. A. (1989), Aerosol, cloud microphysics, and fractional cloudiness, *Science*, *245*, 1227–1230, doi:10.1126/science.245.4923.1227.

Bretherton, C. S., P. N. Blossery, and J. Uchida (2007), Cloud droplet sedimentation, entrainment efficiency, and subtropical stratocumulus albedo, *Geophys. Res. Lett.*, *34*, L03813, doi:10.1029/2006GL027648.

Brioude, J., et al. (2009), Effect of biomass burning on marine stratocumulus clouds off the California coast, *Atmos. Chem. Phys.*, *9*, 8841–8856, doi:10.5194/acp-9-8841-2009.

Coakley, J. A., and C. D. Walsh (2002), Limits to the aerosol indirect radiative effect derived from observations of ship tracks, *J. Atmos. Sci.*, *59*, 668–680, doi:10.1175/1520-0469(2002)059<0668:LTTAIR>2.0.CO;2.

Draxler, R. R., and G. D. Rolph (2003), *HYSPLIT (HYbrid Single-Particle Lagrangian Integrated Trajectory) Model*, Air Resour. Lab., NOAA, Silver Spring, Md.

George, R. C., and R. Wood (2010), Subseasonal variability of low cloud radiative properties over the southeast Pacific Ocean, *Atmos. Chem. Phys.*, *10*, 4047–4063, doi:10.5194/acp-10-4047-2010.

Hill, A. A., and G. Feingold (2009), The Influence of entrainment and mixing assumption on aerosol–cloud interactions in marine stratocumulus, *J. Atmos. Sci.*, *66*, 1450–1464, doi:10.1175/2008JAS2909.1.

Koren, I., L. A. Remer, Y. J. Kaufman, Y. Rudch, and J. V. Martins (2007), On the twilight zone between clouds and aerosols, *Geophys. Res. Lett.*, *34*, L08805, doi:10.1029/2007GL029253.

Lu, M.-L., and J. H. Seinfeld (2005), Study of the aerosol indirect effect by large-eddy simulation of marine stratocumulus, *J. Atmos. Sci.*, *62*, 3909–3932, doi:10.1175/JAS3584.1.

Minnis, P., et al. (2010a), CERES Edition-2 cloud property retrievals using TRMM VIRS and Terra and Aqua MODIS data, part I: Algorithms, *IEEE Trans. Geosci. Remote Sens.*, in press.

Minnis, P., et al. (2010b), CERES Edition-2 cloud property retrievals using TRMM VIRS and Terra and Aqua MODIS data, part II: Examples of average results and comparisons with other data, *IEEE Trans. Geosci. Remote Sens.*, in press.

Painemal, D., and P. Zuidema (2009), Synoptically-induced variability in the microphysical properties of the south east Pacific stratocumulus deck, *Atmos. Chem. Phys. Discuss.*, *9*, 25,523–25,564, doi:10.5194/acpd-9-25523-2009.

Schubert, W. H., J. S. Wakefield, E. J. Steiner, and S. K. Cox (1979), Marine stratocumulus convection. Part I: Governing equations and horizontally homogeneous solutions, *J. Atmos. Sci.*, *36*, 1286–1306, doi:10.1175/1520-0469(1979)036<1286:MSCPIG>2.0.CO;2.

Stevens, B., and G. Feingold (2009), Untangling aerosol effects on clouds and precipitation in a buffered system, *Nature*, *461*, doi:10.1038/nature08281.

Wood, R. (2007), Cancellation of aerosol indirect effects in marine stratocumulus through cloud thinning, *J. Atmos. Sci.*, *64*, 2657–2669, doi:10.1175/JAS3942.1.

B. Albrecht and X. Zheng, Division of Meteorology and Physical Oceanography, Rosenstiel School of Marine and Atmospheric Science, University of Miami, Miami, FL 33149, USA. (xzheng@rsmas.miami.edu)

K. Ayers and P. Minnis, NASA Langley Research Center, Mail Stop 420, 21 Langley Blvd., Hampton, VA 23681, USA.

H. Jonson, Naval Postgraduate School, 3200 Imjin Rd., Hangar 507, Monterey, CA 93933, USA.